Stress transfer relations among the earthquakes that occurred in Kerman province, southern Iran since 1981

Geophys. J. Int. (2006) doi: 10.1111/j.1365-246X.2006.03119.x

Stress transfer relations among the earthquakes that occurred in Kerman province, southern Iran since 1981

Suleyman S. Nalbant, Sandy Steacy and John McCloskey

School of Environmental Sciences, Geophysics Research Group, University of Ulster, Coleraine, BT52 *1SA, Northern Ireland. E-mail: ss.Nalbant@ulster.ac.uk*

Accepted 2006 June 12. Received 2006 June 12; in original form 2006 March 21

SUMMARY

We explore the possible stress triggering relationship of the $M \geq 6.4$ earthquakes that occurred in Kerman Province, southern Iran since 1981. We calculated stress changes due to both coseismic sudden movement in the upper crust and the time-dependent viscous relaxation of the lower crust and/or upper mantle following the event. Four events of $M \geq 6.4$ occurred between 1981 and 2005, on and close to the Gowk fault, show a clear Coulomb stress load to failure relationship. The 2003 $M = 6.5$ Bam earthquake, however, which occurred approximately 95 km SW of the closest Gowk event, shows a very weak stress relation to preceding earthquakes. The coseismic static stress change at the hypocentre of the Bam earthquake is quite small ($\sim$0.006 bars). The time-dependent post-seismic stress change could be 26 times larger or 7 times lower than that of coseismic static stress alone depending on the choice of viscoelastic crustal model and the effective coefficient of friction. Given the uncertainties in the viscoelastic earth models and the effective coefficient of friction, we cannot confidently conclude that the 2003 Bam event was brought closer to failure through coseismic or post-seismic stress loading. Interestingly, the southern Gowk segment with a similar strike to that of the Bam fault, experienced a stress load of up to 8.3 bars between 1981 and 2003, and is yet to have a damaging earthquake.

Key words: Kerman province earthquakes, stress distribution, viscoelasticity.

INTRODUCTION

A number of studies have shown that static stress transfer due to moderate-to-large earthquakes can influence the location and occurrence time of future earthquakes (Harris 1998; Stein 1999; King & Cocco 2001; Steacy *et al.* 2005a) at least in simple tectonic areas such as the North Anatolian fault (Roth 1988; Stein *et al.* 1997), the East Anatolian fault (Nalbant *et al.* 2002), and the Sunda Trench (Nalbant *et al.* 2005a). However, the relation between stress load and triggered seismicity is less clear in tectonically complex areas (Nalbant *et al.* 2005b).

Recent rate-state studies suggest that coseismic stress changes have a time-dependent effect on neighbouring faults with an immediate jump in earthquake probability that decays with time (Parsons *et al.* 2000; Toda & Stein 2002; Toda *et al.* 2005). If the time lag between large events is more than several years then other stress perturbing mechanisms such as interseismic stress accumulation and post-seismic relaxation processes may became important. The occurrence of the 1999 Hector Mine, California earthquake, for example, could not be explained by stress loading due to the 1992 Landers earthquake within the boundaries of the modelling uncertainties (Harris & Simpson 2002). However, its occurrence may be explained by stress loading due to the viscous flow of the lower/upper mantle following the 1992 Landers event (Freed & Lin 2001; Zeng 2001; Pollitz & Sacks 2002), thus demonstrating the potential importance of post-seismic viscoelastic relaxation in stress transfer calculations.

Several mechanisms have been suggested to explain the source of the post-seismic deformation including afterslip on and beneath the rupture, re-equilibration of pore fluid pressure, and viscoelastic relaxation of the lower crust and/or upper mantle (Nur & Mavko 1974; Peltzer *et al.* 1996; Savage & Svarc 1997).

Pore pressure re-equilibration can successfully explain local deformation which occurs in isolated areas along a rupture zone (Peltzer *et al.* 1996, 1998), but cannot explain broader scale deformation. For deformation after a strike-slip event, both afterslip and viscoelastic flow models give similar results and hence there is a debate as to which mechanism is predominantly responsible (Savage 1990; Burgmann *et al.* 2002). However, recent studies involving satellite radar interferometry suggest that viscoelastic flow is required in order to explain longer timescales and wider vertical deformation distributions at the surface (e.g. Fialko 2004; Pollitz *et al.* 2001). Hence we assume that the post-seismic deformation is dominated by the viscoelastic flow in the lower crust or upper mantle.

In the following, we examine coseismic and post-seismic deformation in the Kerman province in southern Iran. This region is interesting in that four successive events with magnitudes larger than

6 in the seismically active north exhibit simple advance to failure relationships whereas the southern region is generally quiescent with the exception of the 2003 Bam earthquake. Below, we first investigate the stress transfer relations in the northern part of the study area, and then focus on the influence of these events on the southern Gowk segment and 2003 Bam rupture plane in the south.

TECTONIC SETTING AND SEISMICITY

The active tectonics of Iran are dominated by the convergence of the Arabian and Eurasian plates which, according to GPS data, occurs at about 22 ± 2 mm/yr in the direction N13°E (Vernant *et al.* 2004). This is ∼10 mm yr^{-1} lower than the rate previously suggested from analysis of global seafloor spreading, fault systems and earthquake slip vectors (DeMets 1994). Deformation and hence seismicity is concentrated at the boundaries of relatively aseismic blocks such as central Iran and Lut (Berberian *et al.* 2001; Walker & Jackson 2002). The Gowk fault is a part of the west side boundary of the Lut block (Fig. 1a), and is oriented NW–SE with a right-lateral strike-slip sense of motion (Fig. 1b). The direction of maximum principal horizontal stress in the area is about N8°E (Vernant *et al.* 2004). The tectonic convergence rate, from GPS measurements, resolved onto this direction is about 8 mm yr^{-1} (Vernant *et al.* 2004), though this rate appears to conflict with the slip rate of the fault zone, 2 mm yr^{-1}, inferred from analysis of geomorphic and drainage features by Walker & Jackson (2002). Within this region the northern segment of the Gowk fault strikes 155° and forms a complex system of fractures and scarps (Walker & Jackson 2002).

The angle of approximately 45° between the regional stress direction and the northern Gowk fault requires a component of shortening. Obvious evidence for this are oblique motion on the Gowk fault with a SW dipping angle, and a series of parallel anticlines associated with a blind thrust, called the Shahdad thrust and fold system, to the east of the Gowk fault (Fig. 1b) (Walker & Jackson 2002). Both the southern branch of the Gowk fault and the Nayband fault to the north are aligned in an almost N–S direction with approximately 10° strike difference with the regional stress. Due to this small angular difference, they have no thrust component.

Although the area has a long record of the damaging historical earthquakes going back about 1000 yr (Ambraseys & Melville 1982), reliable instrumental recordings of seismicity only started in the 1960s. The northern part of the Gowk fault has been quite active since the early 1980s, producing three consecutive $M \geq 6.6$ earthquakes. More recently a moderate size event ($M = 6.4$) occurred NW of the Gowk fault in 2005 February with reverse slip on an approximately E–W striking fault.

To the south, the mapped Bam fault runs parallel to the southern Gowk fault about 45 km east of it (Fig. 1). Unlike the area in which the northern branch of the Gowk fault is located, the area around the southern segment of the Gowk and Bam faults showed no seismic activity prior to the 2003 Bam earthquake. In addition to the instrumental records, historical records (Ambraseys & Melville 1982) show that the southern region did not have a damaging earthquake for more than the last 1000 yr. The best proof for this was the continued existence of the historical mud brick citadel 'Arg-e-Bam'. This citadel, demolished in Bam earthquake, was located at the eastern boundary of the city of Bam and was constructed about 2000 yr ago (Eshghi & Zaré 2003).

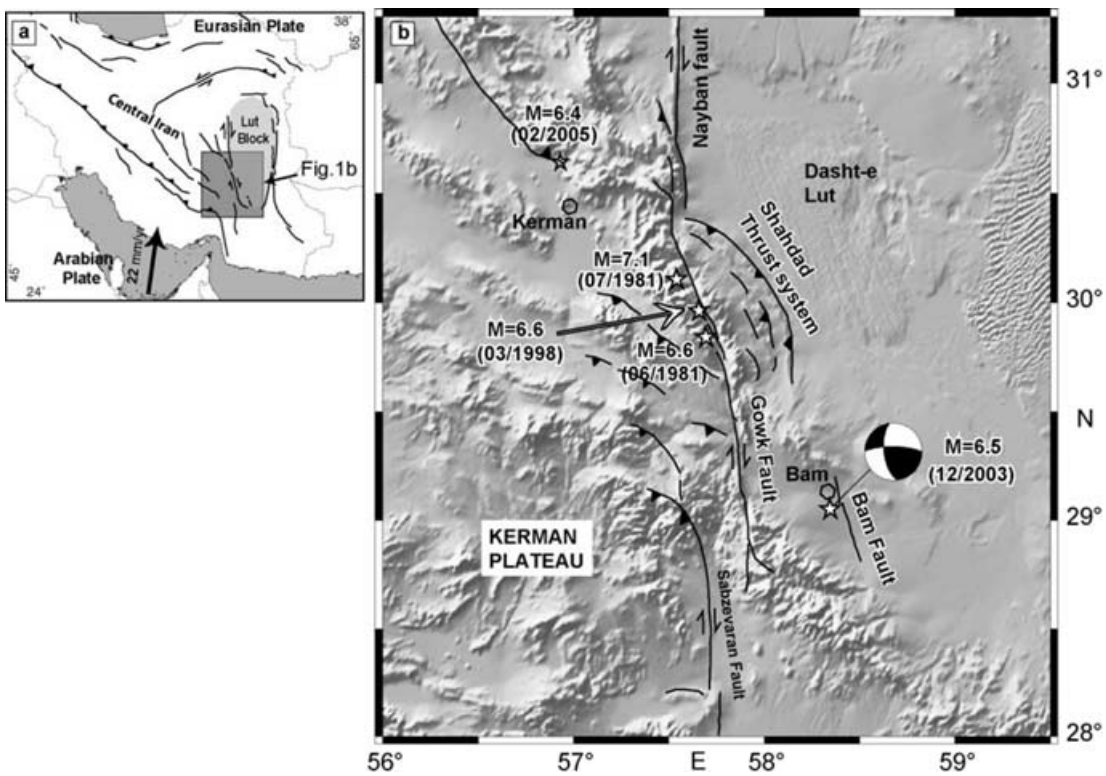

Figure 1. (a) Main tectonic features of Iran. b) Location of the $M \geq 6.4$ earthquakes (based on field observations of Berberian *et al.* 1984, 2001) that occurred on and close to the Gowk fault system within the last century as well as the 2003 and 2005 earthquakes. Faults from Walker & Jackson (2002). Harvard CMT solution for the Bam event is also shown.

Table 1. Earthquakes and faulting parameters that are studied in this paper. The parameters are compiled from Berberian *et al.* (2001) unless otherwise indicated.

Earthquake	Date y/m/d	Magnitude Mw	Length[a] (km)	Width[a] (km)	Strike (°)	Dip (°)	Rake (°)	Mean Slip[b] (m)	Moment ($\times 10^{18}$) N m
Golbaf	1981/06/11	6.6	14.0	15.0	169	52	180	1.4	9.48
Sirch	1981/07/28	7.1	60.0	16.0	157	69	184	2.7	36.69
Fandoqa*	1998/03/14	6.6	22.0	12.4	158	56	195	1.7	9.09
Shahdad**	1998/03/14	—	30.0	20.0	149	6	95	0.08	2.0
Bam	2003/12/26	6.5[c]	20.0	12.0	357[c]	88[c]	−166[c]	Variable[c]	5.8[c]
Zarand	2005/02/22	6.3[d]	15.0	11.0	279[d]	46[d]	124[d]	0.6	3.0[d]

[a]Calculated based on the slip-seismic moment relation of Wells & Coppersmith (1994).
[b]Based on empirical relation of Kanamori & Anderson (1975).
[c]From Talebian *et al.* (2004).
[d]From USGS-NEIC solution.
*This strike-slip event caused unusually large surface slips up to 3 m right lateral and 0.9 m normal slips compared to its size.
**This is the triggered reverse slip on the Shahdad fault system that was recognized by InSAR interferometry (see Figs 1 and 3) (parameters compiled from Berberian *et al.* 2001; Fielding *et al.* 2004; Walker & Jackson 2002).

STUDIED EARTHQUAKES

The earthquakes used in this study are described below and summarized in Table 1.

(i) **1981 June 11, Golbaf earthquake** ($M_w = 6.6$)**:** This event occurred on the northern part of the Gowk fault with a surface rupture of approximately 15 km (Berberian *et al.* 1984). The surface displacements were quite small, typically with 3 cm right-lateral strike-slip and 5 cm vertical. Berberian *et al.* (2001) remodelled the event's focal mechanism solution by using *SH* and *P* waveforms. The focal mechanism indicated right-lateral strike-slip faulting with a small normal faulting component (dipping west) striking NW–SE, parallel to the orientation of the Gowk fault in the area. They had to model the source as two subevents in contrast to the Harvard solution. They suggested a slip of about 75 cm for the first subevent based on the seismic moment (4×10^{18} N m) of it. However, the total seismic moment calculated by them is larger than this as shown in Table 1, thus the total slip has to be larger. In the stress calculation in Section 4 we use slip of 140 cm based on the slip-moment empirical relation of Kanamori & Anderson (1975), $u = Mo/(LWG)$ where L and W are the fault length (km) and down-dip width (km), respectively, and G is the shear modulus (here 3.0×10^{10} N m^{-2}).

(ii) **1981 July 28, Sirch earthquake** ($M_w = 7.1$)**:** The Sirch earthquake occurred on the Gowk fault rupturing a 65 km long section (Berberian *et al.* 1984, 2001). It occurred approximately 1.5 months following the Golbaf event and its southernmost extent was just 6.6 km north of the Golbaf rupture's northern end. It produced right-lateral strike-slip movements up to 50 cm in the north and 25 cm in the south in addition to maximum 40 cm vertical (east side up) surface slip in the north (Berberian *et al.* 2001). Berberian *et al.* (2001) suggested that the almost pure right-lateral strike-slip faulting event experienced 3.3 m average slip by using an empirical relation of displacement to fault length ratio (5×10^{-5}). Here we found it to be 2.7 m from the slip-seismic moment relation of Kanamori & Anderson (1975). We think that the slip-seismic moment relation is more reliable than the empirical relation of displacement to fault length ratio, so we prefer a mean slip 2.7 m for this event.

(iii) **1998 March 14, Fandoqa earthquake** ($M_w = 6.6$)**:** This event occurred between the Golbaf and Sirch events on the Gowk fault. The 23-km-long surface rupture includes re-rupturing of 19 km of the southernmost portion of the Sirch rupture plane and the 6.6 km gap left between the 1981 earthquakes. The focal mechanism studied by seismic waveforms and InSAR interferometry indicates a NW–SE rupture plane dipping to the west with an angle of 50° (Berberian *et al.* 2001). The surface slip distribution was compiled by Berberian *et al.* (2001). Right-lateral slip distribution reaches up to 3 m while the vertical offset comes close to 1 m. Analysing the three events, Berberian *et al.* (2001) speculated on the contrast between the low surface slip distribution due to the 1981 events and the high surface slip distribution caused by the 1998 event and suggested that the main rupture of the 1981 events occurred on deeper parts of the Gowk fault, thus producing only small slip at the surface. Most of the slip occurred at the shallower parts of the same fault parts during the 1998 event, which is supported by the shallow centroid depth from focal mechanism analysis (Berberian *et al.* 2001).

(iv) **March 14, 1998, Shahdad event:** This event or triggered slip has been recognized during the InSAR modelling of the Fandoqa earthquake by Berberian *et al.* (2001). Their InSAR modelling showed that there was a ∼8 cm reverse motion on a very shallow SE dipping (6°) rectangular plane on the Shahdad thrust and folding system in addition to a dominantly right-lateral strike-slip movement on the 1998 Fandoqa rupture plane (Fig. 5) Fielding *et al.* (2004) calculated slips on the Shahdad plane by using a freely slipping boundary element that responded to the 1998 event, and they found approximately 7 cm reverse displacement on the Shahdad rupture plane over area of 30 × 20 km extending from 1 km to 4.5 km below the surface. Both InSAR and boundary element modelling were in good agreement. We, therefore, include this slip in our modelling studies although in practice it has very little influence on the stress change calculations.

(v) **December 26, 2003, Bam earthquake** ($M_w = 6.5$)**:** This event occurred on a blind fault located approximately 4 km west of the previously mapped geologic Bam fault (29.0591°N; 58.3478°E) (Fig. 1b). Envisat radar interferometry and seismic body wave inversion showed that most of the slip was right-lateral, strike-slip on a nearly N–S striking vertical fault (Talebian *et al.* 2004; Wang *et al.* 2004). It caused four discontinuous surface cracks each with typically a few cm slip. From the aftershock distribution and interferometry slip modelling, it was deduced that the length of rupture was about 20 km with a width of 15 km (Nakamura *et al.* 2005; Talebian *et al.* 2004). A right-lateral strike-slip distribution on 2 × 2 km grids was obtained by Talebian *et al.* (2004) with a maximum of 2.5 m slip.

(vi) **2005 February 22, Zarand earthquake** ($M_w = 6.3$)**:** This event occurred approximately 60 km away from the northern end of the rupture plane of the 1981 Sirch event. Both USGS (NEIC) and Harvard gave similar focal mechanism solutions. The horizontal location error is in the range of 5–10 km. The predominantly reverse faulting focal mechanisms define two possible fault planes; both planes striking E–W with a dip toward the north and with a dip toward south. Dip direction and thus the choice of the actual rupturing plane from the USGS_NEIC solution is inferred from the careful inspection of topographic and tectonic features in the area, so a rupture plane with a strike 279, with a dip angle of 46° to the north is preferred.

CALCULATION OF EARTHQAUKE STRESS CHANGES

We calculate both coseismic and post-seismic stress changes due to the earthquakes. We use Okada's (1992) code for coseismic stress calculations and treat the Earth as a homogeneous elastic half-space and faults as rectangular dislocations embedded within it. For the post-seismic stress changes due to relaxation in the viscoelastic lower crust and upper mantle in response to the faulting in the elastic upper crust, we use a stratified earth model and employ the code VISCO1D (Pollitz 1992). It calculates post-seismic relaxation by separating displacement fields into their toroidal and spheroidal components and evaluates them using modal summation on an spherically symmetric earth. It uses a linear (Maxwell) rheology for viscoelastic layers and also incorporates the effect of medium compressibility.

To assess how a fault or the rupture plane of target event has been brought closer or away from the failure due to the preceding earthquakes, we use the Coulomb failure function, $\Delta\sigma_f = \Delta\tau + \mu' \Delta\sigma_n$ where $\Delta\sigma_f$, $\Delta\tau$ and $\Delta\sigma_n$ are the change in Coulomb stress, shear and normal stresses on the target plane, respectively. The shear stress change is calculated in the slip direction of the target fault and normal stress is positive if the fault is unclamped. μ' represents the apparent coefficient of friction which includes the unknown effect of pore pressure change and is believed to range between 0.2 and 0.8 depending on pore fluid content of the fault zone. It could be as low as 0.2 in well developed and repeatedly ruptured fault zones because of the thick impermeable gouge material developed in the fault zone that trap pore fluids in the zone causing the sliding friction to drop (Scholz 1990; Stein 1999). On the other hand it could be as high as 0.8 in young minor faults, since they did not have enough displacement to develop such a gouge material. We choose μ' to be 0.6 in our illustrations, although in general the choice of μ' is not crucial (King *et al.* 1994; Steacy *et al.* 2004, 2005). For example, our results for Gowk fault earthquakes changes only in detail for end members of μ'. In the case of the Bam earthquake the choice of it is important because the stress loads on the Bam rupture are so low. We, therefore, examine results for the Bam event for varying μ' between 0.2 and 0.8.

Both coseismic and post-seismic stress changes are resolved onto the faults in the region and onto the fault planes of subsequent earthquakes. Any positive changes in Coulomb stress are interpreted as faults brought close to failure. We do not make any distinction between the influences of the same amount of coseismic and post-seismic stress changes on the target fault, though rate change calculations based on rate-state friction predict an elevated impact due to the coseismic stress changes compared to the post-seismic or secular stress changes (e.g. Toda *et al.* 2005).

PARAMETERS OF THE EARTH MODEL FOR POST-SEISMIC CALCULATIONS

To be able to model the post-seismic deformation with viscoelastic flow, one needs to know the viscoelastic earth stratification. There are two end-member models of the controlling viscoelastic earth structure. The first model consists of a weak (i.e. low-viscosity) lower crust and strong upper mantle. For example a study of Brace & Kohlstedt (1980) on the structure of the crust, examining the depth distribution of earthquakes and extrapolating laboratory rock mechanics experiments to a geological scale, gave a picture of this model that was called the 'jelly sandwich model' (Jackson 2002). This earth model has been used in numerous numerical modelling studies, such as Deng *et al.* (1998, 1999) and Freed & Lin (2001). However, recent studies show that deformations over longer time periods and in broader regions are better explained by the upper mantle flow model (Pollitz *et al.* 2001) and favour a strong lower crust-weak upper mantle structure at least in California (i.e. Pollitz *et al.* 2000). This second earth model, the strong lower crust–weak upper mantle, is also supported by accurately located earthquake hypocentral location and gravitational data as argued by Jackson (2002).

As there have been no studies related to the rheology of the lower crust in this area that could help us to constrain viscosities we include both end-member earth models in our viscoelastic relaxation calculations by considering plausible viscosity limits.

Studies based on modelling of post-seismic geodetic data show that the viscosity of the substrata below the brittle upper crust could range between 10^{17} and 10^{20} Pa s (Deng *et al.* 1998; Pollitz *et al.* 2000; Hearn *et al.* 2002; Freed & Lin 2001; Bürgmann *et al.* 2002). We adopt viscoelastic earth models from previous studies mentioned above which have typical rheology appropriate for the continental crust (Fig. 2). Based on the strength of the viscous lower and upper mantle layers, we refer to them as VE1 and VE2. The model VE1 has a weak lower crust (viscosity, $\eta_{lc} = 10^{18}$ Pa s) and strong upper mantle (viscosity, $\eta_m = 10^{20}$ Pa s, Fig. 2a). In contrast, VE2 has a strong lower crust (viscosity, $\eta_{lc} = 10^{20}$ Pa s) and weak upper mantle layers (viscosity, $\eta_m = 10^{19}$ Pa s) (Fig. 2b). In addition, other possible viscosities are considered in calculations of the stress changes at the hypocentre of the Bam event.

RESULTS

Fig. 3(a) shows the Coulomb stress change following the first event (June 11, 1981, $M = 6.6$) of the Gowk earthquake sequence. Coulomb stress changes are calculated at 2 km spacing along the mapped active structures with full regard to their 3-D orientations and slip directions at 8 km depth (i.e. Nalbant *et al.* 2002). Coulomb stress changes are also mapped onto the rupture plane of the 1981 Sirch event ($M = 7.1$), which are positive over almost the entire rupture plane with a maximum value of about 2 bars (Fig. 3b). A 6.6 km long gap was observed on the surface between the rupture planes of two 1981 events (Berberian *et al.* 2001). Although they couldn't explain why this gap was left, our stress change calculations clearly show that most of the area experienced a stress decrease due to the first 1981 earthquake. This gap experiences a stress increase from the second 1981 event (Fig. 4) and is filled by the future 1998 event, which was the third large event in the sequence.

Note that the southern extension of the Gowk fault toward the town of Sarvestan is also loaded by about 3.4 bars due to the first Gowk event.

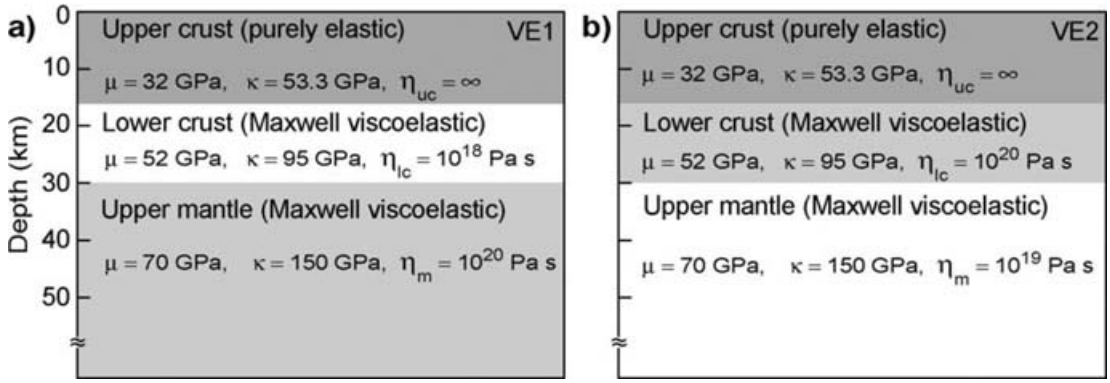

Figure 2. The structure of two-end member earth models for viscoelastic relaxation calculations. Here μ, κ, and η represent shear modulus, bulk modulus and viscosity, respectively.

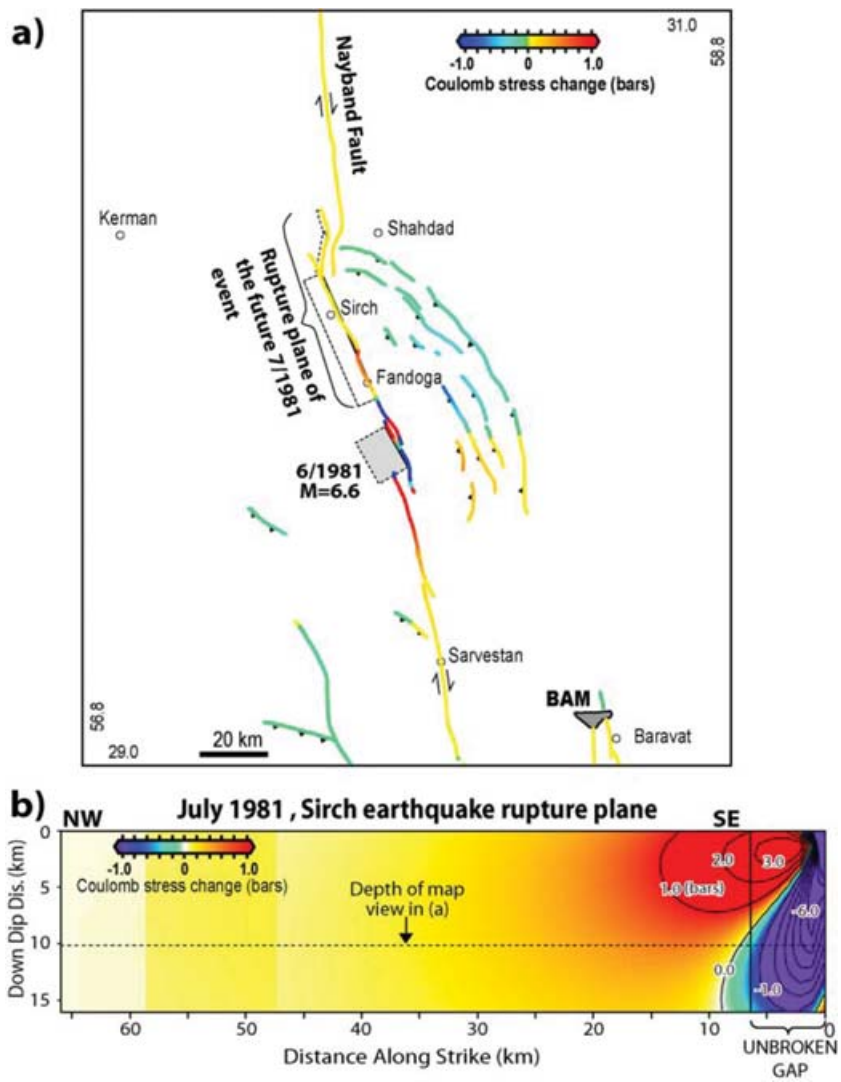

Figure 3. Coulomb stress change on the faults due to the 1981 June event at 8 km depth plotted on the surface trace of the faults (a), and a cross-section of the stress change over the rupture plane of the future Sirch (1981 July) event (b). Note the stress shadow over most of the area that did not participate in the July earthquake. This is likely the primary reason why this patch was left unbroken. Note that in this and following figures the surface projections of the ruptured planes are shown by grey filled rectangles. Future rupture planes are represented by transparent rectangles. The dashed lines indicate the edges of the planes at depth.

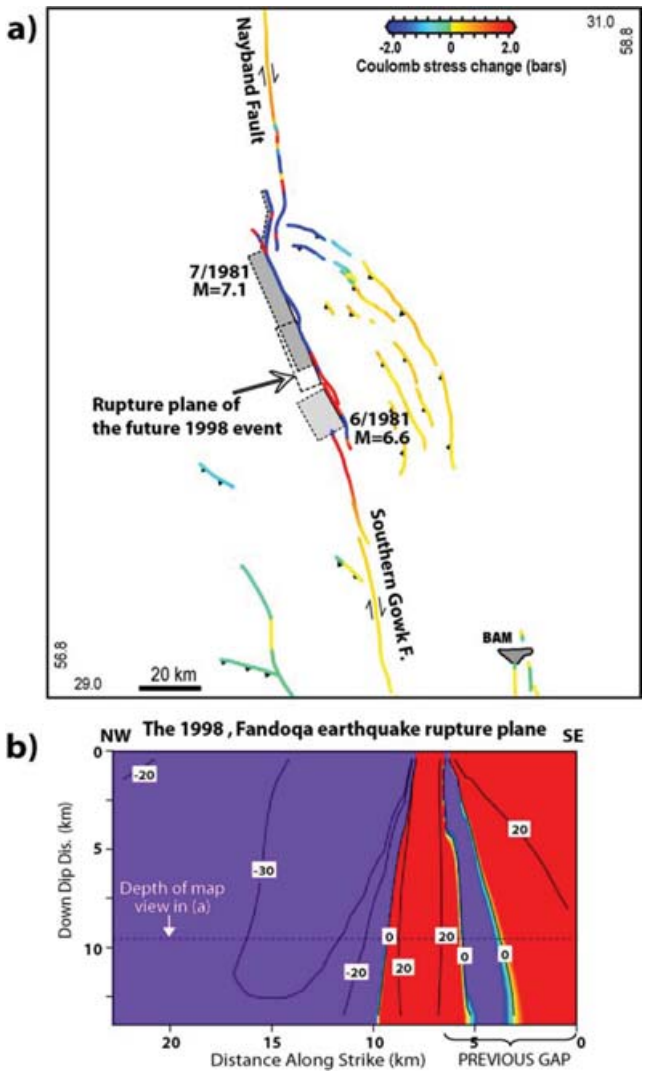

Figure 4. Coulomb stress change on the faults due to the Gowk events occurred in 1981 at 8 km depth (a) and over the rupture plane of the 1998 Fandoga earthquake (b).

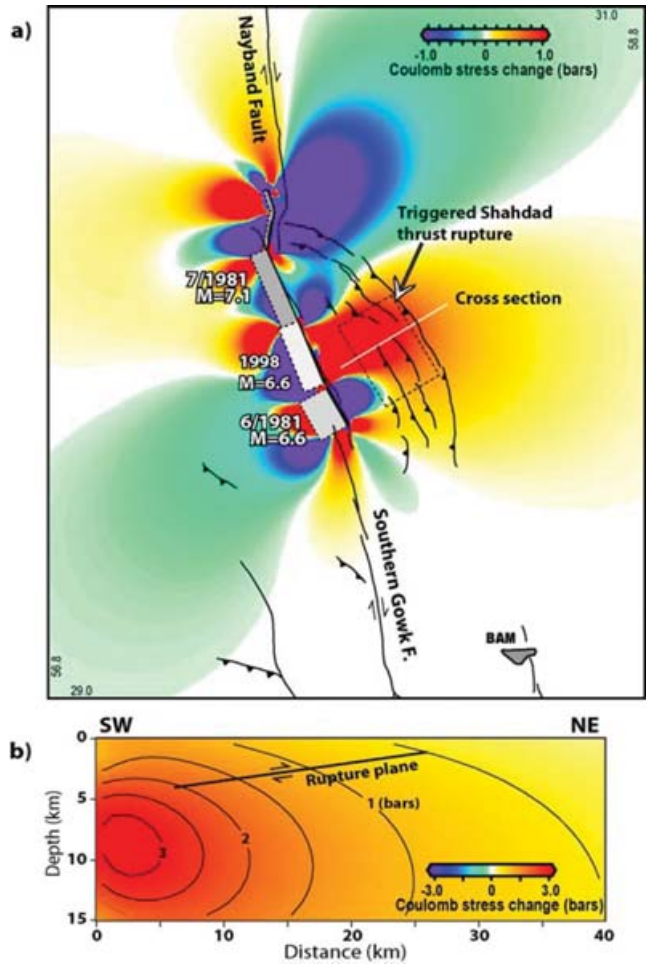

Figure 5. Coulomb stress change at a depth of 3 km on 6°SW dipping reverse faults striking parallel to the triggered Shahdad fault caused by the previous three Gowk events (a). Cross-section along the white line over the Shahdad thrust system (b). Note the strong stress loading from 0.5 to 2 bars on the rupture plane.

Fig. 4(a) shows the combined Coulomb stress change resulting from the first two events of the sequence. The stress field across the rupture plane of the 1998 event is also shown in Fig. 4(b). A part of the southern section of the Sirch event (17 km out of 60 km) is re-ruptured during the 1998 Fandoga event (Berberian *et al.* 2001). Although this overlapping part of the previous Sirch event has large negative stress change, other areas on the plane have positive stress change up to 20 bars. In addition to the coseismic increase, during the 17 yr there were viscoelastic stress increases at the hypocentre ranging from 1.5 to 7.4 bars depending on the choice of the viscoelastic models VE2 and VE1, respectively.

The extent of the triggered Shahdad rupture plane is shown in Fig. 5(a). Coseismic Coulomb stress change on the surface of the Shahdad plane due to the Gowk sequence events is positive over almost the entire plane and in the cross-section ranges from 0.5 to 2 bars (Fig. 5b). As discussed by Berberian *et al.* (2001) and Fielding *et al.* (2004) this shallow movement must have happened between the dates (1996 and 1998) of acquisition of the images that used for the interferometry. It is most likely that it occurred following the 1998 Fandoga event, and our modelling result supports this (Fig. 5).

Fig. 6(a) shows coseismic Coulomb stress change in the wider region due to the Gowk fault earthquakes discussed above. The stress change over the future Bam rupture plane is also shown below. The magnitude of the stress change at the hypocentre of the Bam event was about 0.006 bars for our chosen value of $\mu' = 0.6$ while on the most of the rupture plane it ranges from 0.0 to 0.028 bars. This becomes about -0.004 bars if μ' is chosen to be 0.2 (minimum -0.02 and maximum 0.016 bars over the plane). These are clearly well below the previously suggested aftershock stress-triggering threshold of 0.1 bars (Reasenberg & Simpson 1992; King *et al.* 1994), though other authors report no lower limit for the triggering (i.e. Ziv & Rubin 2000). The total stress changes (coseismic + post-seismic) at the time of the Bam earthquake are shown in Figs 6(b) and (c) for the VE1 and VE2 models, respectively, with post-seismic contributions alone over the Bam rupture plane. The stress transfer to the upper crust is stronger in the VE1 model than it is in the VE2 model. Considering both models, the stress load changes are between 0.04 and 0.052 bars, significantly larger than that of the coseismic load alone.

We explore the sensitivity of these results by altering the viscosity of the lower crust (η_{lc}) in the VE1 model but keeping viscosity of the upper mantle and other elastic parameters the same. In the VE2

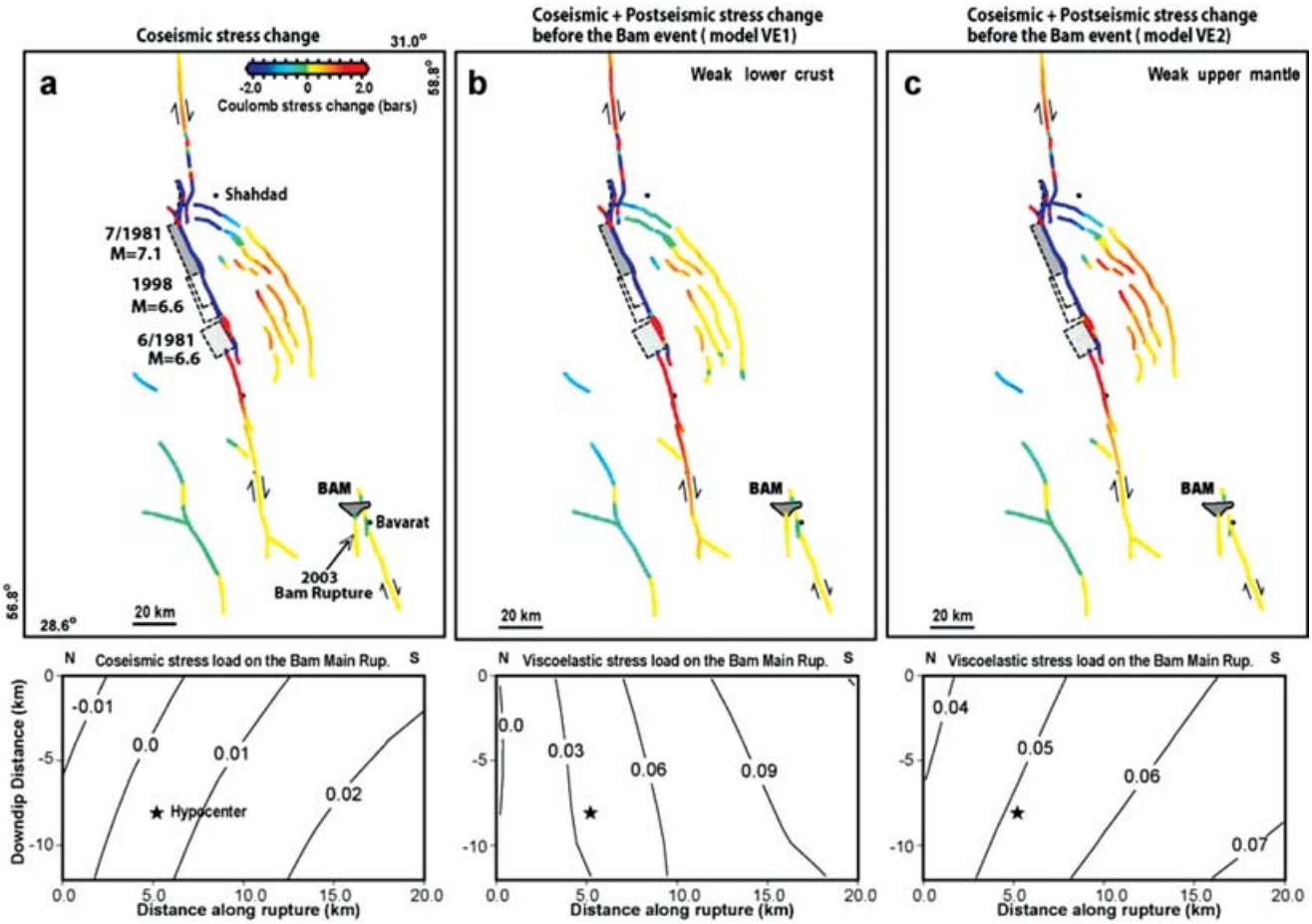

Figure 6. (a) Coseismic stress change, (b) combined (coseismic + post-seismic) stress change for viscoelastic earth model VE1 and (c) for viscoelastic earth model VE2, due to the three large events that occurred on the Gowk fault system (see Table 1 for faulting parameters). The apparent coefficient of friction μ' 0.6 is used for the calculations. The stress changes across the main Bam rupture plane (strike = 357°, dip = 88° and rake = −166° given by Talebian *et al.* 2004) is shown below for coseismic and viscoelastic contributions separately. Note the very small stress load for all models.

Table 2. The effect of different viscosities of viscous layers in the viscoelastic models on Coulomb stress calculations at the hypocentre of the Bam earthquake. Other elastic parameters are kept constant.

VE1 Model ($\eta_{\rm m}$ = 10E+20 Pa s constant)			VE2 Model ($\eta_{\rm lc}$ = 10E+20 Pa s constant)		
Name	Viscosity ($\eta_{\rm lc}$) (Pa s)	CSH* (bars)	Name	Viscosity ($\eta_{\rm m}$) (Pa s)	CSH.* (bars)
VE1_1	10E+17	0.16	VE2_1	10E+17	0.085
VE1_2	10E+18	0.03	VE2_2	10E+18	0.053
VE1_3	10E+19	−0.07	VE2_3	10E+19	0.048

*Coulomb stress change at the hypocentre.

model we changed the viscosity of upper mantle (η_m) and kept other parameters constant (Table 2) for the same purpose. These calculations are undertaken at the hypocentre of the Bam event (for $\mu' =$ 0.6). The Coulomb stress changes range from −0.07 to 0.16 bars, depending on the choice of viscoelastic earth model and viscosities. This means that the contribution of the post-seismic viscoelastic relaxation could be as large as 26 times greater than the coseismic only (∼0.006 bars).

In order to assess the effect of μ' on our results, we calculate Coulomb stress change at the hypocentre of the Bam earthquake for various μ' ranging from 0.2 to 0.8. The results for the viscoelastic and coefficient of friction variations are shown in Fig. 7.

As can be seen from Fig. 7, the weaker the viscoelastic strata, the higher the Coulomb stress loading at the hypocentre. This loading reaches its highest value, 0.22 bars in the VE1_1 earth model with the $\mu' = 0.8$. The stress change at the hypocentre is negative in the earth model VE1_3 regardless of the value of μ' (lowest value −0.95 bars with $\mu' = 0.8$). As mentioned earlier this might be expected since the 2003 rupture plane is located at the edge between the positive and negative stress lobes. Given this sensitivity to the earth models, it is impossible to conclude that viscoelastic relaxation played an important role in the occurrence of the 2003 Bam event.

The Fig. 8(a) shows both the coseismic (a) and post-seismic (b) (for the earth model VE1) stress changes on the planes parallel to

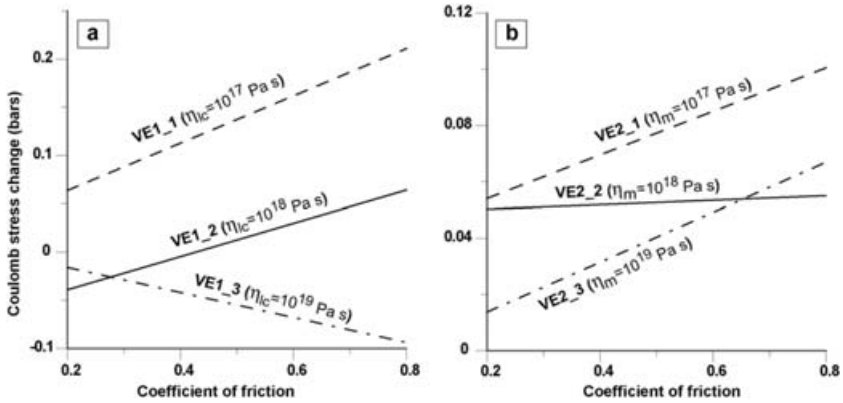

Figure 7. Coulomb stress change at the hypocentre of the 2003 Bam earthquake for different viscoelastic models with different values of the apparent coefficient of friction. For modelling parameters and naming conventions see Table 2.

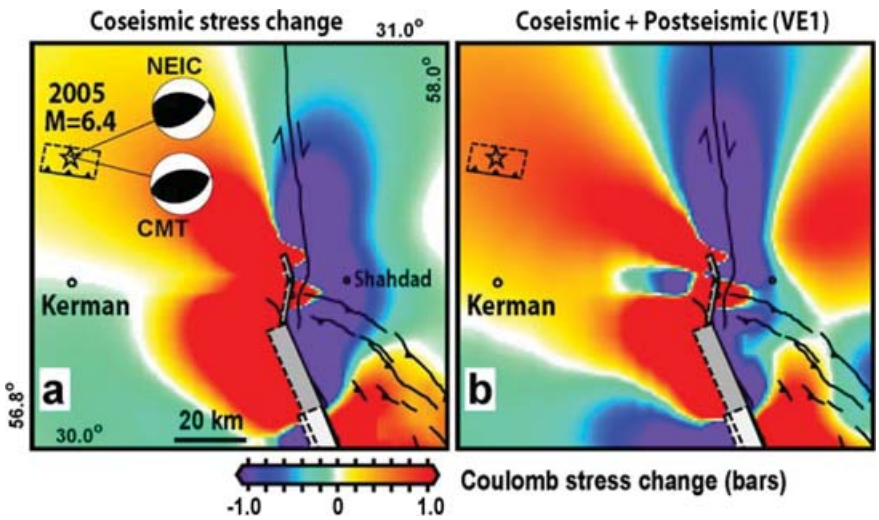

Figure 8. Coulomb stress change in the region of the February 22, 2005 event due to the Gowk events (resolved at 8 km depth). The stress is calculated on the orientation of the nodal plane (strike 279°, dip 46° and rake 129°) given by USGS-NEIC which is consistent with the regional topography and tectonics. (a) Coseismic and (b) combined (coseismic + post-seismic) Coulomb stress changes before the 2005 event.

that of the 2005 event at 8 km depth which is close to the suggested centroid depth by USGS (NEIC). The stress change at the hypocentral area increased from 0.2 bars coseismic load to 0.9 bars at the time of earthquake with the viscoelastic relaxation of the lower crust. The 2005 fault plane was clearly brought closer to failure by the preceding Gowk fault events.

DISCUSSION AND CONCLUSION

We investigate the stress interaction relationship among the $M \geq 6.4$ events that occurred in the Kerman Province, southern Iran since 1981. The three Gowk fault events show clear stress load to failure relationships. A coseismic Coulomb stress load of up to 2 bars due to the first 1981 event appears to have had a significant influence on the occurrence time of the second 1981 event. The third, 1998, event in the sequence started in the gap left between the 1981 events and re-ruptured a considerable part of the second 1981 fault. The 6.6 km of unbroken fault that was left between the two 1981 events may be explained by a strong Coulomb stress decrease over most of that segment. A similar reason was speculated for the rupture extent of the 1992 Big Bear earthquake ($M = 6.5$) by King *et al.* (1994). It occurred approximately 3.5 hr following the 1992 Landers earthquake, and its rupture was located in a stress increased lobe caused by the Landers event. The authors suggested that the rupture terminated where the stress change became negative. Although the controls on rupture propagation are clearly complex and whether any particular area of a fault fails in a specific event depends on its previous stressing history (secular and coseismic), here it appears that the high stress decreases from the first 1981 event led to the termination of rupture of the second 1981 earthquake leaving the 6.6 km gap. Subsequent positive coseismic stress may have overcome this stress decrease, permitting the occurrence of the 1998 event. Additional positive coseismic stress load due to the 1981 Sirch event and post-seismic loading over 17 yr may have helped overcome the stress shadow.

The combined Coulomb stress changes with a maximum value of 0.9 bars at the hypocentral area of the 2005 Kerman event appear to have advanced it towards failure. Similarly the stress field generated by all the three Gowk fault events explains the triggered deformation on the Shahdad thrust and fold zone as captured by the SAR interferometry (i.e. Berberian *et al.* 2001).

The occurrence of 2003 Bam earthquake was anomalous in that it occurred in a seismically quiet area compared to its surroundings. Interestingly the rupture was located at the edge of a positive stress

lobe and received very little stress load both from either coseismic (0.006 bars at the hypocentre) or post-seismic stress changes due to the preceding Gowk earthquakes.

It is also worth emphasizing that all the three Gowk fault earthquakes occurred on the N155E striking northern segment of the fault. No significant event has been recorded on the more steeply striking (∼N175°E) southern Gowk segment and on the Nayband fault (striking ∼N177°E) during the instrumental time period. When we consider the maximum regional stress direction which is N8°E ±5° in the area, we may conclude that most of the regional or secular strain is taken up by the northern Gowk fault segment. The Nayband fault to the north and the southern Gowk fault are both aligned very close to the direction of the regional stress which may cause very little strain accumulation and hence lead to a much longer earthquake occurrence period. This might be an explanation for the lack of moderate to large events on these faults. However, the occurrence of the Bam earthquake on a buried N177°E striking fault suggest that these slowly stressing N–S are still capable of experiencing damaging earthquakes. The southern Gowk segment may hence be of concern as it has received a coseismic stress increase of up to 5.4 bars and a viscoelastic stress increase between 0.4 (VE2) and 2.9 bars (VE1).

ACKNOWLEDGMENTS

We thank the editor, Thorsten Becker, Karen Felzer, and an anonymous reviewer for constructive comments that improved the manuscript. We also thank Fred Pollitz for allowing us to use his viscoelastic deformation code and kindly answering many questions and Mehrdad Mostafazadeh for the earthquake catalogue of Iran and his help.

REFERENCES

Ambraseys, N. & Melville, C., 1982. *A History of Persian Earthquakes*, Cambridge University Press, Cambridge.

Berberian, M., Jackson, J.A., Ghorashi, M. & Kadjar, M.H., 1984. Field and teleseismic observations of the 1981 Golbaf–Sirch earthquakes in SE Iran. *Geophys. J. R. astr. Soc.,* **77**, 809–838.

Berberian, M. et al., 2001. The 14 March 1998 Fandoqa earthquake (Mw 6.6) in Kerman province, S.E. Iran: re-rupture of the 1981 Sirch earthquake fault, triggering of slip on adjacent thrusts, and the active tectonics of the Gowk fault zone, *Geophys. J. Int.,* **146,** 371–398.

Bürgmann, R., Ergintav, S., Sagall, P., Hearn, E.H., McClosky, S., Reilinger, R.E., Woith, H. & Zschau, J., 2002. Time-dependent distributed afterslip on and deep below the Izmit rupture, *Bull. seism. Soc. Am.,* **92,** 126–137.

Brace, W.F. & Kohlstedt, D.L., 1980. Limits of lithospheric stress imposed by laboratory experiments, *J. geophys. Res.,* **85,** 6348–6252.

DeMets, C., 1994. Effect of recent revisions to the geomagnetic reversal time scale on estimates of current plate motions, *Geophys. Res. Lett.,* **21,** 2191–2194.

Deng, J., Gurnis, M., Kanamori, H. & Hauksson, E., 1998. Viscoelastic flow in the lower crust after the 1992 Landers, California, earthquake, *Science,* **282,** 1689–1692.

Deng, J., Hudnut, K., Gurnis, M. & Hauksson, E., 1999. Stress loading from viscous flow in the lower crust and triggering of aftershocks following the 1994 Northridge, California, Earthquake, *Geophys. Res. Lett.,* **26**(21), 3209–3212, doi:10.1029/1999GL010496.

Eshghi, S. & Zaré, M., 2003. Bam (SE Iran) earthquake of 26 December 2003, Mw6.5: a Preliminary Reconnaissance Report, http://www.iiees.ac.ir/English/bam_report_english_recc.html.

Fialko, Y., 2004. Evidence of fluid-filled upper crust from observations of postseismic deformation due to the 1992 Mw7.3 Landers earthquake, *J. geophys. Res.,* **109,** B08401, doi:10.1029/2004JB002985.

Fielding, E.J., Wright, T.J., Muller, J., Parsons, B.E. & Walker, R., 2004. Aseismic deformation of a fold-and-thrust belt imaged by synthetic aperture radar interferometry near Shahdad, southeast Iran, *Geology,* **32,** 577–580.

Jackson, J., 2002. Strength of the continental lithosphere: time to abandon the jelly sandwich? *GSA Today,* **12,** 4–10, doi:10.1130/1052-5173.

Freed, A.M. & Lin, J., 2001. Delayed triggering of the 1999 Hector Mine earthquake by viscoelastic stress transfer, *Nature,* **411,** 180–183.

Hearn, E.H., Bürgmann, R. & Reilinger, R.E., 2002. Dynamics of Izmit earthquake postseismic deformation and loading of the Duzce earthquake hypocenter, *Bull. seism. Soc. Am.,* **92,** 172–193.

Harris, R.A., 1998. Stress triggers, stress shadows, and implications for seismic hazard, *J. geophys. Res.,* **103,** 24 347–24 358.

Harris, R.A. & Simpson, R.W., 2002. The 1999 M_w 7.1 Hector Mine, California, earthquake: a test of the stress shadow hypothesis?, *Bull. seism. Soc. Am.,* **92,** 1497–1512.

Kanamori, H. & Anderson, D.L., 1975. Theoretical basis of some empirical relations in seismology, *Bull. seism. Soc. Am.,* **65,** 1073–1095.

King, G.C.P. & Cocco, M., 2001. Fault interaction by elastic stress changes: New clues from earthquake sequences, *Adv. Geophys.,* **44,** 1–38.

King, G.C.P., Stein, R.S. & Lin, J., 1994. Static stress changes and the triggering of earthquakes, *Bull. seism. Soc. Am.,* **84,** 935–953.

Nakamura, T. et al., 2005. Source fault structure of the 2003 Bam earthquake, southeastern Iran, inferred from the aftershock distribution and its relation to the heavily damaged area: Existence of the Arg-e-Bam fault proposed, *Geophys. Res. Lett.,* **32,** L09308, doi:10.1029/2005GL022631.

Nalbant, S.S., McCloskey, J., Steacy, S. & Barka, A.A., 2002. Stress accumulation and increased seismic risk in eastern Turkey, *Earth planet. Sci. Lett.,* **195,** 291–298.

Nalbant, S.S., Steacy, S., Sieh, K., Natawidjaja, D. & McCloskey, J., 2005a. Earthquake risk on the Sunda Trench, *Nature,* **435,** 756–757.

Nalbant, S.S., McCloskey, J. & Steacy, S., 2005b. Lessons on the calculation of static stress loading from the 2003 Bingol, Turkey earthquake, *Earth planet. Sci. Lett.,* **235,** 632–640.

Nur, A. & Mavko, G., 1974. Postseismic viscoelastic rebound, *Science,* **183,** 204–206.

Okada, Y., 1992. Internal deformation due to shear and tensile faults in a half-space, *Bill. seism. Soc. Amer.,* **82,** 1018–1040.

Parsons, T., Toda, S., Stein, R.S., Barka, A. & Dieterich, J.H., 2000. Heightened Odds of Large Earthquakes Near Istanbul: an Interaction-Based Probability Calculation, *Science,* **288,** 661.

Peltzer, G., Rosen, P., Rogez, F. & Hudnut, K., 1996. Postseismic rebound in fault step-overs caused by pore fluid flow, *Science,* **273,** 1202–1204.

Peltzer, G., Rosen, P., Rogez, F. & Hudnut, K., 1998. Poro-elastic rebound along the Landers 1992 earthquake surface rupture, *J. geophys. Res.,* **103,** 30 131–30 145.

Pollitz, F.F., 1992. Postseismic relaxation theory on the spherical Earth, *Bull. seism. Soc. Am.,* **82,** 422–453.

Pollitz, F.F. & Sacks, I.S., 2002. Stress triggering of the 1999 Hector Mine earthquake by transient deformation following the 1992 Landers earthquake, *Bull. seism. Soc. Am.,* **92,** 1487–1496.

Pollitz, F.F., Peltzer, G. & Bürgmann, R., 2000. Mobility of continental mantle: Evidence from postseismic geodetic observations following the 1992 Landers earthquake, *J. geophys. Res.,* **105,** 8035–8054.

Pollitz, F.F., Wicks, C. & Thatcher, W., 2001. Mantle Flow Beneath a Continental Strike-Slip Fault: Postseismic Deformation After the 1999 Hector Mine Earthquake, *Science,* **293,** 1814–1818.

Reasenberg, P.A. & Simpson, R.W., 1992. Response of regional seismicity to the static stress change produced by the Loma Prieta earthquake, *Science,* **255,** 1687–1690.

Roth, F., 1988. Modelling of stress patterns along the western part of the North Anatolian fault zone, *Tectonophysics,* **152,** 215–226.

Savage, J.C., 1990. Equivalent strike-slip earthquake cycles in half-space and lithosphere-asthenosphere Earth models, *J. geophys. Res.,* **95,** 4873–4879.

Savage, J.C. & Svarc, J.L., 1997. Postseismic deformation associated with the 1992 *Mw* 7.3 Landers earthquake, southern California, *J. geophys. Res.,* **102,** 7565–7577.

Scholz, C.H., 1990. *The Mechanics of Earthquakes and Faulting*, Cambridge University Press, Cambridge.

Steacy, S., Marsan, D., Nalbant, S.S. & McCloskey, J., 2004. Sensitivity of static stress calculations to the earthquake slip distribution, *J. geophys. Res.,* **109,** B04303, doi:10.1029/2002JB002365.

Steacy, S., Gomberg, J. & Cocco, M., 2005a. Introduction to special section: Stress transfer, earthquake triggering, and time-dependent seismic hazard, *J. geophys. Res.,* **110,** B05S01, doi:10.1029/2005JB003692.

Steacy, S., Nalbant, S.S., McCloskey, J., Nostro, C., Scotti, O. & Baumont, D., 2005b. Onto what planes should Coulomb stress perturbations be resolved?, *J. geophys. Res.*, doi:10.1029/2004JB003356.

Stein, R.S., 1999. The role of stress transfer in earthquake occurrence, *Nature,* **402,** 605–609.

Stein, R.S., Barka, A.A. & Dieterich, J.H., 1997. Progressive failure on the North Anatolian fault since 1939 by earthquake stress triggering, *Geophys. J. Int.,* **128,** 594–604.

Talebian, M. *et al.*, 2004. The 2003 Bam (Iran) earthquake: Rupture of a blind strike-slip fault, *Geophys. Res. Lett.,* **31,** L11611, doi:10.1029/2004GL020058.

Toda, S. & Stein, R.S., 2002. Response of the San Andreas fault to the 1983 Coalinga-Nunez earthquakes: An application of interaction-based probabilities for Parkfield, *J. geophys. Res.,* **107**(B6), 2126, doi:10.1029/2001JB000172.

Toda, S., Stein, R., Richards-Dinger, K. & Bozkurt, S., 2005. Forecasting the evolution of seismicity in southern California: Animations built on earthquake stress transfer, *J. geophys. Res.,* **110,** B05S16, doi:10.1029/2004JB003415.

Vernant, P.F. *et al.*, 2004. Present day Crustal Deformation and Plate Kinematics in Middle East Constrained by GPS measurements in Iran and Northern Oman, *Geophys. J. Int.,* **157,** 381–398.

Walker, R. & Jackson, J.A., 2002. Offset and evolution of the Gowk Fault, S.E. Iran: A major intra-continental strike-slip system, *J. Struct. Geol.,* **24,** 1677–1698.

Wang, R., Xia, Y., Grosser, H., Wetzel, H.-U., Kaufmann, H. & Zschau, J., 2004. The 2003 Bam (SE Iran) earthquake: precise source parameters from satellite radar interferometry, *Geophys. J. Int.,* **159,** 917–922, doi:10.1111/j.1365-246X.2004.02476.x.

Wells, D.L. & Coppersmith, K.J., 1994. New empirical relationships among magnitude, rupture length, rupture width, rupture area, and surface displacement, *Bull. seism. Soc. Am.,* **84,** 974–1002.

Ziv, A. & Rubin, A.M., 2000. Static stress transfer and earthquake triggering; no lower threshold in sight?, *J. geophys. Res.,* **105,** 13 631–13 642.

Zeng, Y.H., 2001. Viscoelastic stress-triggering of the 1999 Hector Mine earthquake by the 1992 Landers earthquake, *Geophys. Res. Lett.,* **28,** 3007–3010.